View metadata, citation and similar papers at core.ac.uk
brought to you by CORE
provided by Elsevier - Publisher Connector

Available online at www.sciencedirect.com
SCIENCE DIRECT®
Physics Letters B 633 (2006) 195–200
PHYSICS LETTERS B
www.elsevier.com/locate/physletb

Dark matter search experiment with CaF_2(Eu) scintillator at Kamioka Observatory

Y. Shimizu [a,*], M. Minowa [a,b], W. Suganuma [a,1], Y. Inoue [c]

[a] *Department of Physics, School of Science, University of Tokyo, 7-3-1, Hongo, Bunkyo-ku, Tokyo 113-0033, Japan*
[b] *Research Center for the Early Universe (RESCEU), School of Science, University of Tokyo, 7-3-1, Hongo, Bunkyo-ku, Tokyo 113-0033, Japan*
[c] *International Center for Elementary Particle Physics (ICEPP), University of Tokyo, 7-3-1, Hongo, Bunkyo-ku, Tokyo 113-0033, Japan*

Received 29 September 2005; received in revised form 28 November 2005; accepted 12 December 2005

Available online 19 December 2005

Editor: L. Rolandi

Abstract

We report recent results of a WIMP dark matter search experiment using 310 g of CaF_2(Eu) scintillator at Kamioka Observatory. We chose a highly radio-pure crystal, PMTs and radiation shields, so that the background rate decreased considerably. We derived limits on the spin dependent WIMP-proton and WIMP-neutron coupling coefficients, a_p and a_n. The limits excluded a part of the parameter space allowed by the annual modulation observation of the DAMA NaI experiment.

© 2005 Elsevier B.V. Open access under CC BY license.

PACS: 14.80.Ly; 29.40.Mc; 95.35.+d

Keywords: Scintillation detector; Calcium fluoride; Dark matter; WIMP

1. Introduction

There is substantial evidence that most of the matter in our Galaxy must be dark matter that exists in the form of weakly interacting massive particles (WIMPs) [1]. WIMPs are thought to be non-baryonic particles, and the most plausible candidates for them are the lightest supersymmetric particles. WIMPs can be directly detected through elastic scattering with nuclei in radiation detectors. Using various detectors, many groups have performed experiments for the detection of WIMPs.

For the direct WIMP detection, two kinds of interactions need to be considered: the axial-vector (spin-dependent, SD) interaction and the scalar (spin-independent, SI) interaction. WIMPs couple to the spin of the target nuclei in the SD interaction while they coherently couple to almost all nucleons of the target nuclei in the SI interaction. For the SD interaction, ^{19}F is one of the most favorable nuclei to detect WIMPs because of its large nuclear spin and 100% natural abundance. Furthermore, the spin expectation values of protons and neutrons in ^{19}F have the opposite signs while those values in other nuclei usually have the same signs [2–6]. Therefore, experiments with a ^{19}F-target can set complementary limits to those with nuclei whose spins have the same sign.

Several direct WIMP searches using ^{19}F-based detectors, such as bolometers [7,8], scintillators [9,10] and superheated droplet detectors (SDDs) [11,12], have already been performed. Our group had also carried out WIMP search experiments using LiF and NaF bolometers [7,8]. Although these results set complementary limits to those of NaI(Tl) experiments, the background rates below 20 keV could not be decreased sufficiently. The sources of the main background were thought not to be any radiation but to be intrinsic and instrumental noises in the bolometers. As an alternative method, we have carried out experiments using CaF_2(Eu) scintillators. CaF_2(Eu) is known as a useful scintillator for WIMP searches because of its high light yield (19 000 photons/MeV) and has already been used in sev-

---

[*] Corresponding author.
E-mail address: pikachu@icepp.s.u-tokyo.ac.jp (Y. Shimizu).

[1] Now at Third Research Center, Technical Research and Development Institute, Japan Defence Agency, 1-2-10, Sakae, Tachikawa, Tokyo 190-8533, Japan.

0370-2693 © 2005 Elsevier B.V. Open access under CC BY license.
doi:10.1016/j.physletb.2005.12.025

eral experiments. However, these experiments show rather high background rates ($\gtrsim 10$ counts/k.e.e./day/kg [2]) in comparison with the NaI(Tl) experiments (~ 1 counts/k.e.e./day/kg). In addition, its light yield is about 50% of NaI(Tl), so that the energy threshold of CaF_2(Eu) detectors is higher than NaI(Tl) detectors. Therefore, these CaF_2(Eu) experiments set less stringent limits to the SD interaction than the NaI(Tl) experiments. In order to reduce the background rates and to improve the energy threshold of our experiments, we have tried to eliminate radioactive sources of γ-rays and studied detection efficiency near the energy threshold.

In this Letter, the results of our new experiment with a CaF_2(Eu) scintillator are presented.

2. Experimental setup

The detector consisted of a CaF_2(Eu) crystal with a mass of 310 g. It was installed in Kamioka Observatory (2700 m.w.e.). To reduce the background, low radioactive PMTs (Hamamatsu R8778) and a low radioactive radiation shield were used. The experimental setup is shown in Fig. 1. The crystal was produced from the same stock of CaF_2 raw powder as used by the CANDLES experiment [14] and low radioactive EuF_3 powder. The low radioactive PMT was developed by the XMASS experiment [13] and thought to be the least radioactive among available PMTs. Two PMTs were attached to the crystal through 5 cm-long quartz light guides. The photoelectron yield of the scintillator was about 4 photoelectrons/k.e.e. at 60 k.e.e. The radiation shield consisted of 5 cm of highly pure copper (99.9999%), 10 cm of OFHC copper, 15 cm of lead, and 20 cm of polyethylene. The highly pure copper was supplied by Mitsubishi materials. The whole setup was separated from the mine air by two layers of EVOH sheet [15] so that radon gas in the air could not come into the detector. The radon free air generated in Kamioka Observatory was sent into the detector as shown in the figure. In addition, the radon concentration around the detector was continuously monitored by a radon detector. It was kept at about 30 mBq/m^3 throughout the experiment.

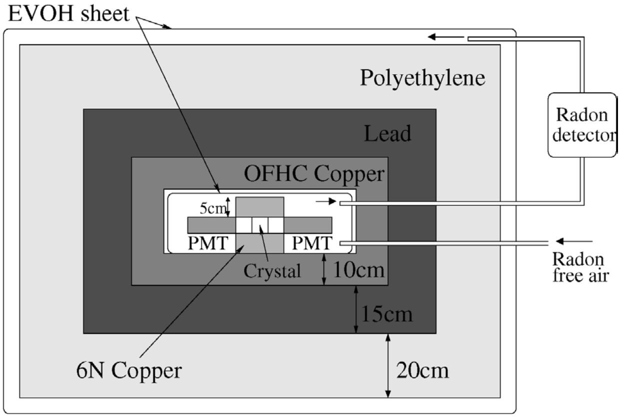

Fig. 1. Schematic view of the experimental setup.

For the data acquisition, a dual trace digital oscilloscope was used to record wave forms of PMT pulses. The pulses of each PMT are directly sent to the oscilloscope without any amplifier then daisy-chained to a trigger system with a tee connector. The impedance of each oscilloscope input was set to 1 MΩ and the cables are terminated at the inputs of the trigger system. The wave forms were digitized at the oscilloscope at a rate of 1 GS/s for a total digitization time of 10 μs and sent to a PC for an off-line analysis.

In the trigger system, the pulses were amplified by PMT amplifiers and sent to low threshold discriminators. Thresholds of the discriminators were set to 1/4 of the mean pulse hight of single photoelectron events. The single photoelectron events were obtained by irradiating the PMT with continuous feeble light from an LED. The detection efficiency of each PMT with the discriminator threshold for a single photoelectron event was obtained to be 0.8 by comparing the discriminator output counts and the total number of single photoelectron events; the latter was estimated by assuming a normal distribution for the charge distribution of the single photoelectron events. Parameters of the normal distributions were determined in a special measurements by recording the events with low-threshold internal triggers of the oscilloscope to include the low energy tail of the spectrum. The charge distribution of the internally triggered events was well fitted by the normal distribution. Single counting rates of PMTs were typically 20 Hz.

The discriminator signals were then sent to the coincidence circuit. It generated a trigger pulse for the oscilloscope when both of the PMTs gave signals in coincidence within 1 μs. It reduced the number of background events due to dark noise of the PMTs.

The trigger efficiency of the data acquisition system was calculated as a function of a number of photoelectrons by the Monte Carlo analysis. In this analysis, we generated a certain number of photoelectrons in a time sequence according to the scintillation decay time of CaF_2(Eu). The probability that each scintillation photon reaches to each PMT is assumed to be the same. The detection probability of a photoelectron was set to 0.8. Then, we measured an interval between arbitrary photoelectrons of each PMT in the event. The fraction of events that generated at least one output signal in both of the discriminators within 1 μs was taken to be the trigger efficiency. At 2 k.e.e., 8 photoelectrons were generated and the trigger efficiency was calculated to be 0.93. Threshold energy for the following analysis was set at 2 k.e.e.

3. Measured spectra

The WIMP observation was carried out from March to May 2005. Measured spectra are shown in Fig. 2. The energy scale is defined by calibration with 60 keV γ-rays from ^{241}Am assuming the number of photoelectron is proportional to the energy. A bump around 50 k.e.e. is found in Fig. 2. It is caused by ^{152}Eu radioactivity in the crystal which is generated by the neutron activation on the ground. To see the response in the low energy

---

[2] In this Letter, we use the unit k.e.e. or keV electron equivalent for nuclear recoil energy since the scintillation efficiency for nuclear recoils is less than electron recoils due to high ionization loss.

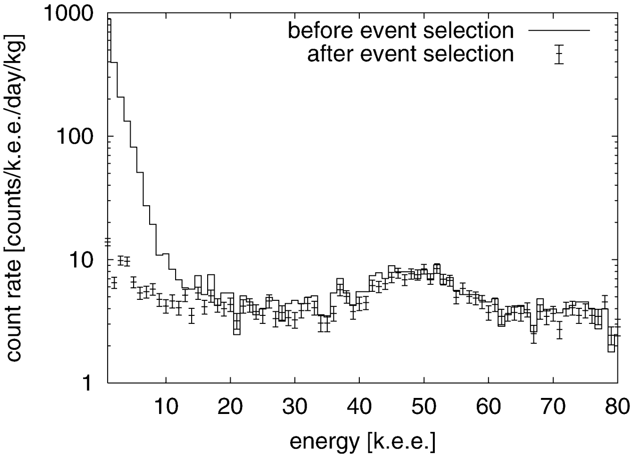

Fig. 2. Measured spectra before and after the event selection is applied. The energy scale is normalized to a calibration point of 60 keV electron recoil.

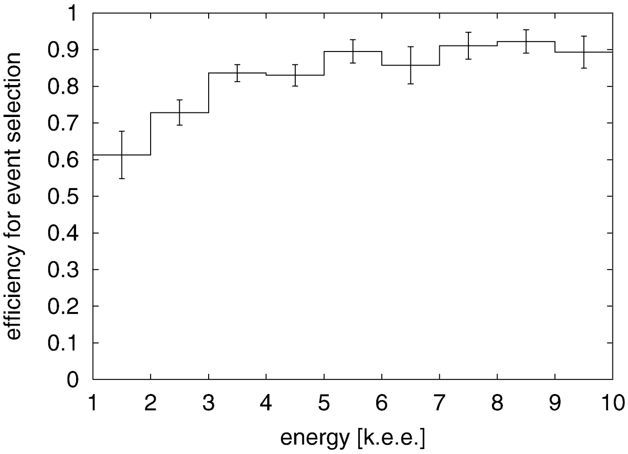

Fig. 3. Estimated efficiency for the event selection.

region, we measured a spectrum of 5.9 keV X-rays with ^{55}Fe. The rms energy resolution was 34%.

In the energy region below 10 k.e.e., background events due to Cherenkov photons dominate the event rates. The Cherenkov events were produced in the light guides by Compton electrons caused by background γ-rays. We used a pulse shape discrimination (PSD) technique to eliminate these events. Cherenkov photons are observed as fast pulses (<10 ns) while scintillation photons as slow pulses (~1 µs). Therefore, we used the ratio of the integral charge of the partial pulse shape period (0–30 ns) to that of the total pulse shape period (0–10 µs) as a discrimination parameter in the off-line analysis. To set the discrimination cut, we compared low energy scintillation events which cannot produce Cherenkov photons (obtained using 122 keV γ-rays from ^{57}Co) and Cherenkov events (obtained using 1133 and 1333 keV γ-rays from ^{60}Co). In addition, we eliminate events in which observed charge of the two PMTs shows high asymmetry because they are thought to be the remaining Cherenkov events or electric noise events. To estimate the efficiency of the off-line event selection, the low energy scintillation events were used. We calculated a fraction of the scintillation events which remained after the selection as a function of energy (Fig. 3). Consequently, the event selection reduced the count rates to less than 10 counts/k.e.e./day/kg in the energy region between 2 and 10 k.e.e.

4. Limits on the WIMP-nucleon interaction

Using the measured spectrum, limits on the SD WIMP-nucleon interaction were derived. The limits were calculated using the same manner as described in Ref. [16]. To derive the upper limits, we conservatively assumed all events to be nuclear recoils caused by the WIMP scattering. The astrophysical and nuclear parameters used to obtain the limits are listed in Table 1. Only the contribution of ^{19}F was considered while ^{40}Ca had negligible contribution to the SD interaction because ^{40}Ca consisted of even protons and even neutrons. The scintillation efficiency f_q of the ^{19}F recoil in a CaF$_2$(Eu) was measured by other experiments [17,25,26]. Although all of these experiments show that the scintillation efficiency tends to increase in lower energy region, we choose conservatively a constant value $f_q = 0.11$. As was done in Ref. [17], ^{19}F recoil energy is calculated with f_q and the interpolated energy scale between 0 and 60 k.e.e.:

Table 1
Astrophysical and nuclear parameters used to obtain the limits

Astrophysical parameters	
Dark matter density	0.3 GeV/cm^3
Velocity distribution	Maxwellian
Velocity dispersion	220 km/s
Solar system velocity	232 km/s
Nuclear parameters of ^{19}F	
Total spin	$\frac{1}{2}$
Spin expectation value of protons	0.441
Spin expectation value of neutrons	−0.109

$$E_N = \frac{L}{L_{60\ \text{keV}}} \frac{60[\text{keV}]}{f_q}, \tag{1}$$

where E_N is the ^{19}F recoil energy and L is the scintillation yield of an event.

For the SD interaction, the WIMP-nucleus cross section is written as

$$\sigma^{SD}_{\chi\text{–N}} = \frac{32 G_F^2 \mu^2_{\chi\text{–N}}}{\pi} \left(a_p \langle S_{p(N)}\rangle + a_n \langle S_{n(N)}\rangle\right)^2 \frac{J+1}{J}, \tag{2}$$

where G_F is the Fermi coupling constant, $\mu_{\chi\text{–N}}$ is the WIMP-nucleus reduced mass, $\langle S_{p(N)}\rangle$ and $\langle S_{n(N)}\rangle$ are the expectation values of the proton and neutron spins within the nucleus and J is the total nuclear spin [18].

The upper limit of the WIMP-nucleus scattering cross section $\sigma^{SD}_{\lim\,\chi\text{–N}}$ is obtained by the experiment. From Eq. (2), limits in the a_p–a_n plane is written with $\sigma^{SD}_{\lim\,\chi\text{–N}}$:

$$\left(a_p \langle S_{p(N)}\rangle + a_n \langle S_{n(N)}\rangle\right)^2 \frac{J+1}{J} < \frac{\pi \sigma^{SD}_{\lim\,\chi\text{–N}}}{32 G_F^2 \mu^2_{\chi\text{–N}}}. \tag{3}$$

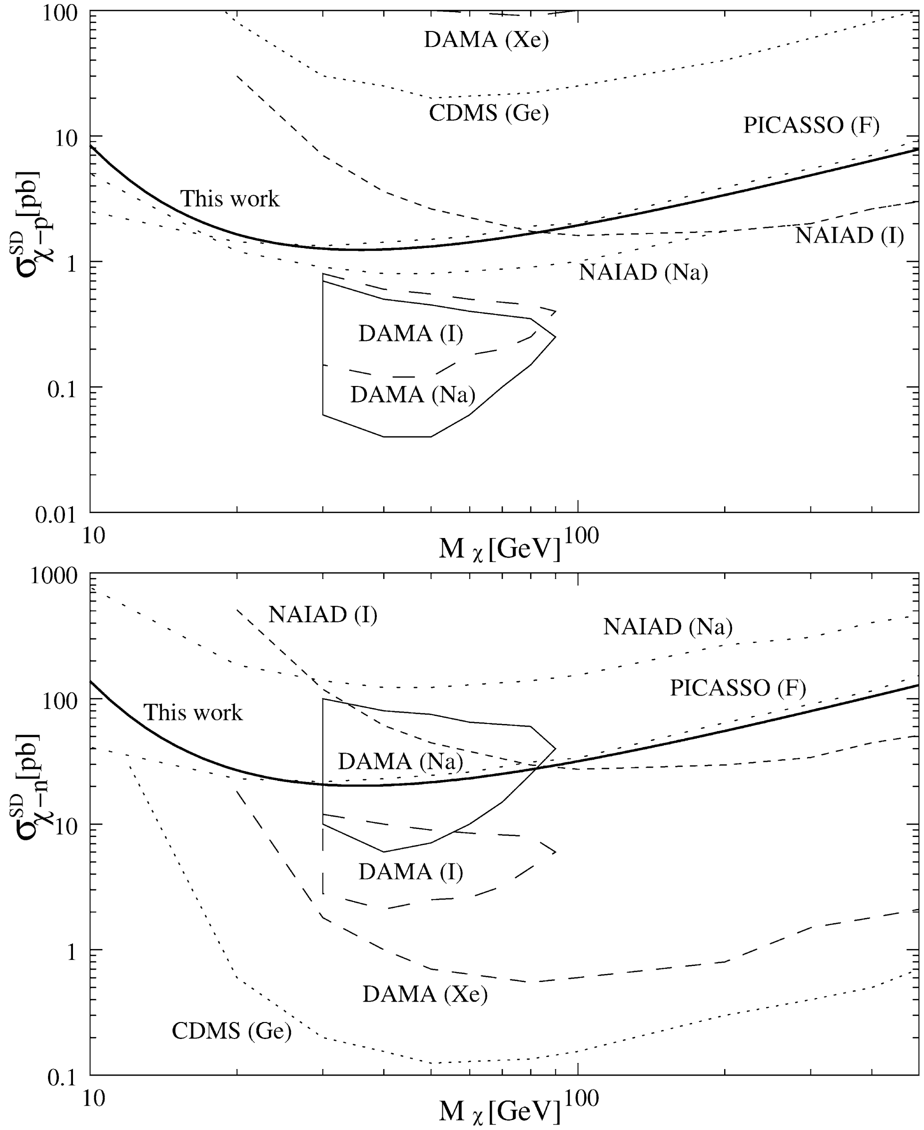

Fig. 4. Recent limits on the SD WIMP-proton cross section and WIMP-neutron cross section. Results of NAIAD [20], PICASSO [12], CDMS [21], DAMA NaI [22,24], DAMA Xe [23] and our experiments are shown.

As in Ref. [19], limits on a single nucleon interaction are generally calculated:

$$\sigma^{\mathrm{SD}}_{\lim\,\chi-\mathrm{p(N)}} = \sigma^{\mathrm{SD}}_{\lim\,\chi-\mathrm{N}} \frac{\mu^2_{\chi-\mathrm{p}}}{\mu^2_{\chi-\mathrm{N}}} \frac{\langle S_\mathrm{p}\rangle^2}{\langle S_{\mathrm{p(N)}}\rangle^2} \frac{J+1}{J},$$
$$\sigma^{\mathrm{SD}}_{\lim\,\chi-\mathrm{n(N)}} = \sigma^{\mathrm{SD}}_{\lim\,\chi-\mathrm{N}} \frac{\mu^2_{\chi-\mathrm{n}}}{\mu^2_{\chi-\mathrm{N}}} \frac{\langle S_\mathrm{n}\rangle^2}{\langle S_{\mathrm{n(N)}}\rangle^2} \frac{J+1}{J}, \qquad (4)$$

where $\langle S_\mathrm{p}\rangle = \langle S_\mathrm{n}\rangle = \frac{1}{2}$, $\sigma^{\mathrm{SD}}_{\lim\,\chi-\mathrm{p(N)}}$ and $\sigma^{\mathrm{SD}}_{\lim\,\chi-\mathrm{n(N)}}$ are the WIMP-proton and WIMP-neutron scattering cross section limits when $a_\mathrm{n}\langle S_{\mathrm{n(N)}}\rangle = 0$ and $a_\mathrm{p}\langle S_{\mathrm{p(N)}}\rangle = 0$ in Eq. (3), respectively. Fig. 4 shows $\sigma^{\mathrm{SD}}_{\lim\,\chi-\mathrm{p(N)}}$ and $\sigma^{\mathrm{SD}}_{\lim\,\chi-\mathrm{n(N)}}$ derived from our experiment as a function of WIMP mass M_χ. Results of other experiments are also shown in the figure.

The limits in the a_p–a_n plane for WIMP mass $M_\chi = 50$ and 200 GeV are shown in Fig. 5. The limits of other experiments are also shown. The outside of the two solid lines is excluded by our experiment. The region between the two ellipses is allowed by the annual modulation observation of the DAMA experiment [24]. Our results exclude a part of the DAMA allowed region by means of odd-proton target. Experiments with odd-neutron targets such as the CDMS [21] also set similar limits. Our results are comparable to the recent results of PICASSO [12] experiment which uses SDDs of fluorocarbon, C_4F_{10}. Recently, we became acquainted with a new result from the SIMPLE Collaboration [27] which was very similar to our present result.

5. Conclusion

The WIMP search experiment using 310 g of CaF_2(Eu) was carried out. The highly pure copper shield and the quartz light guides were used to eliminate γ-rays from the outer materials. Pulse shape discrimination effectively eliminated Cherenkov events, which dominated the count rates below 10 k.e.e. As a result, count rates were lower than 10 counts/k.e.e./day/kg between 2 and 10 k.e.e. We obtained the limits on the WIMP-

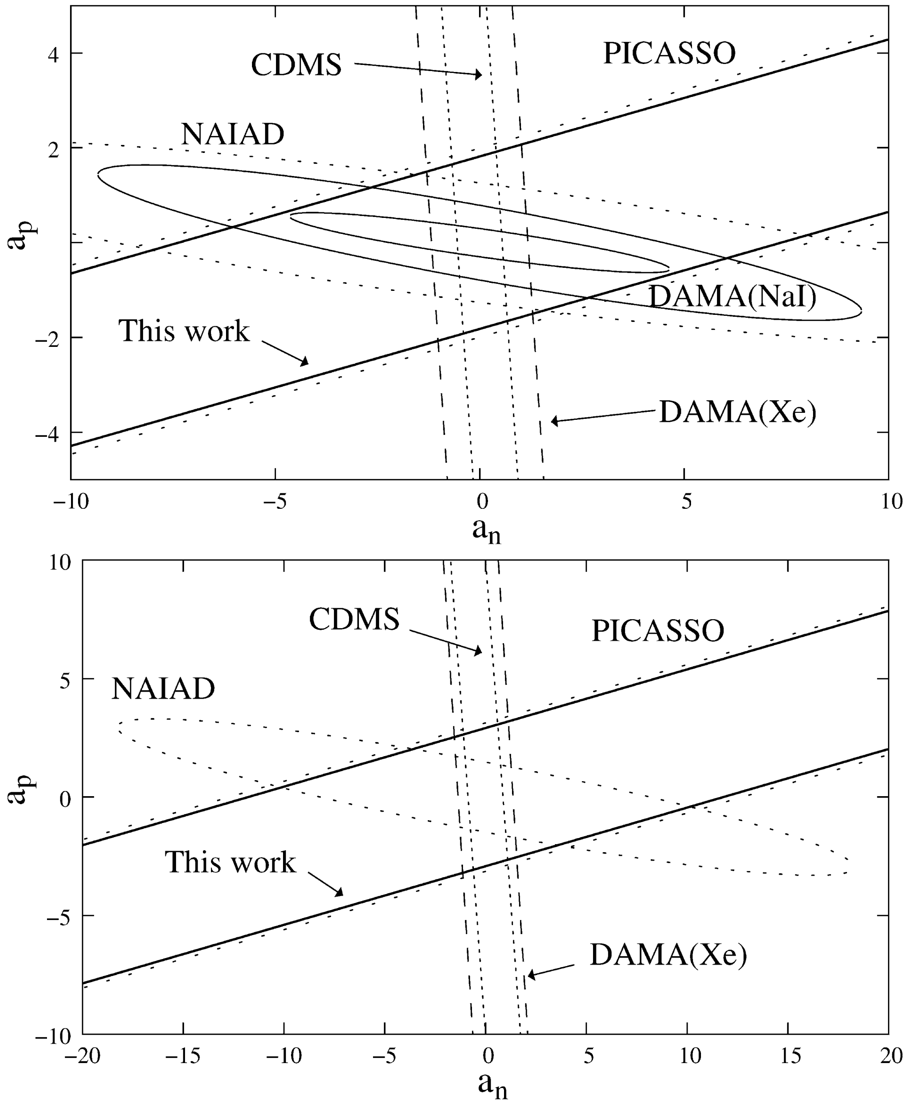

Fig. 5. Limits in the a_p–a_n plane for $M_\chi = 50$ GeV (upper) and 200 GeV (lower). The region between two solid lines is allowed by this experiment. Results of NAIAD [20], PICASSO [12], CDMS [21], DAMA NaI [22,24] and DAMA Xe [23] experiments are also shown.

nucleon spin dependent interaction in terms of the WIMP-nucleon coupling coefficients a_p and a_n. Our results excluded a part of the parameter region allowed by the annual modulation measurement by the DAMA NaI experiment.

Acknowledgements

We would like to acknowledge the help of the staff of Kamioka Observatory, Institute for Cosmic Ray Research, University of Tokyo in performing this experiment. We want to express our thanks to XMASS Collaboration for allowing us to obtain the low radioactive PMT R8778 based on their development. We also want to express our thanks to Prof. T. Kishimoto of CANDLES Collaboration for allowing us to obtain the low background CaF_2(Eu) crystal based on the low background CaF_2(pure) they developed. This research is supported by Research Center for the Early Universe, School of Science, University of Tokyo.

References

[1] G. Jungman, M. Kamionkowski, K. Griest, Phys. Rep. 267 (1996) 195.
[2] J. Engel, S. Pittel, E. Ormand, P. Vogel, Phys. Lett. B 275 (1992) 119.
[3] J. Engel, S. Pittel, P. Vogel, Int. J. Mod. Phys. E 1 (1992) 1.
[4] M.T. Ressell, et al., Phys. Rev. D 48 (1993) 5519.
[5] J. Engel, et al., Phys. Rev. C 52 (1995) 2216.
[6] M.T. Ressell, D.J. Dean, Phys. Rev. C 56 (1997) 535.
[7] K. Miuchi, et al., Astropart. Phys. 19 (2003) 135.
[8] A. Takeda, et al., Phys. Lett. B 572 (2003) 145.
[9] R. Bernabei, et al., Astropart. Phys. 7 (1997) 73;
R. Belli, et al., Nucl. Phys. B 563 (1999) 97.
[10] I. Ogawa, et al., Nucl. Phys. A 663 (2000) 869c.
[11] F. Giuliani, et al., Phys. Lett. B 588 (2004) 151.
[12] M. Barnabe-Heider, et al., hep-ex/0502028.
[13] S. Moriyama, et al., in: Proceedings of International Workshop on Technique and Application of Xenon Detectors (Xenon01), World Scientific, Singapore, 2001.
[14] S. Yoshida, et al., Nucl. Phys. B (Proc. Suppl.) 138 (2005) 214;
S. Umehara, et al., in: Proceedings of Symposium on Neutrinos and Dark Matter in Nuclear Physics (NDM03), in press.
[15] http://www.kuraray.co.jp/en/index.html.

[16] J.D. Lewin, P.F. Smith, Astropart. Phys. 6 (1996) 87.
[17] D.R. Tovey, et al., Phys. Lett. B 433 (1998) 150.
[18] J. Ellis, et al., Phys. Lett. B 481 (2000) 304.
[19] D.R. Tovey, et al., Phys. Lett. B 488 (2000) 17.
[20] B. Ahmed, et al., Astropart. Phys. 19 (2003) 691.
[21] D. Akerib, et al., Phys. Rev. Lett. 93 (2004) 211301.
[22] R. Bernabei, et al., Phys. Lett. B 509 (2001) 197.
[23] R. Bernabei, et al., Phys. Lett. B 436 (1998) 379.
[24] F. Giuliani, T.A. Girard, Phys. Rev. D 71 (2005) 123503.
[25] G.J. Davies, et al., Phys. Lett. B 332 (1994) 159.
[26] R. Hazama, et al., Nucl. Instrum. Methods A 482 (2002) 297.
[27] T.A. Girard, et al., Phys. Lett. B 621 (2005) 233.